Geomechanics and Geotechnics: From Micro to Macro – Jiang et al. (eds)
© 2011 Taylor & Francis Group, London, ISBN 978-0-415-61295-1

Bimodal character of induced anisotropy in granular materials under undrained shear

Ning Guo & Jidong Zhao
Department of Civil and Environment Engineering, Hong Kong University of Science and Technology, Hong Kong, P.R. China

ABSTRACT: Granular anisotropy is attributable to many complex behaviors of granular materials and reflects important microstructures at the grain scale, and should be fully considered towards the development of realistic constitutive models for such materials. In this paper, we present a study on the behavior of anisotropy using a three-dimensional Discrete Element Method (DEM). Isotropic packings of sand with different initial states are sheared to large strain under undrained conditions. The bimodal character of force transmission and induced anisotropy in the granular assembly is carefully examined. Under some conditions, such as when liquefaction occurs, it is found that certain degree of geometric anisotropic may develop in the weaker-than-average force network, wherein the mechanical anisotropy remains largely small. The study helps to improve our understanding on granular materials, and will be useful for geotechnical applications.

Keywords: granular materials, DEM, anisotropy, bimodal character, liquefaction

1 INTRODUCTION

Under external loads, granular materials such as sand exhibit complex behavior involving anisotropy, dilatancy, pressure and density dependence, combined isotropic and kinematic hardening, and transitional solid-liquid state such as liquefaction. Anisotropy has been found to play a key role in many of these aspects and should be included in the constitutive modeling of granular materials (see. i.e., Li and Dafalias, 2002; Jefferies and Been, 2006). The current state of research on this topic, however, is much limited by the availability of efficient experimental tools and approaches to identify anisotropy and its evolution during complex loading paths (Mitchell and Soga, 2005). The use of grain-scale-based numerical tools such as the Discrete Element Method (DEM) has been a popular alternative in helping us improve our understanding on granular anisotropy (Cundall and Strack, 1979; Oda and Iwashita, 2000).

DEM studies reveal that forces in granular materials are transmitted through inter-particle contacts, and their distribution is strongly inhomogeneous in most case. In particular, the stress transmission in confined granular material subjected to shear has been found to exhibit an interesting bimodal phenomenon (Radjai et al., 1998, 2004) using 2D DEM with disk-like particles. The forces have been found to belong to two distinct classes which contribute differently to anisotropy, stress, and dissipation: a long-bearing percolating network of force contacts carrying a force larger than the average force (the strong network), and a dissipative network of contacts carrying a force smaller than the average (the weak network). During shear, the whole deviatoric load is supported by the strong force chains, while the dissipative weak network contributes only to the average pressure. Anisotropy has been closely correlated with this special feature of force network during the loading process. This numerical finding has been further confirmed by recent experiments on photo-elastic particles (i.e., Majumdar and Behringer, 2005). The bimodal feature observed by Radjai and coworkers, however, has been mainly based on 2D DEM simulations. Their more recent research using 2D pentagonal particles (Azema et al., 2007) has led to slightly different conclusions, e.g., with respect to the development of anisotropy in the weak network.

In this paper, we present some preliminary results on the study of anisotropic sand behavior. The bimodal character will be carefully examined by using a 3D DEM code with polydisperse sphere particles. In this code, the rotation of particles is fully taken into account by considering the frictional resistances to relative motion between particles. All samples will be prepared to reach an initially isotropic state such that the behavior of induced anisotropy can be investigated without the needing to consider inherent anisotropy in the material.

2 APPROACH AND FORMULATION

The three-dimensional DEM employed here is similar to that used by Abe et al., (2004) and Wang and Alonso-Marroquin (2009). A linear Hookean contact model is employed to describe the inter-particle contact. The normal and tangential stiffness of the particles, as input parameters, can be estimated by similar ways as used by Sitharam et al., (2009). A packing of 16,000 particles with polydisperse radius ranged between 0.2 mm and 0.6 mm is adopted in the study. A vertical loading speed of 1.0×10^{-6}/s is used to ensure quasi-static conditions and meanwhile the lateral strain rate is adjusted so as to keep the total volume constant, as such undrained condition is maintained. Table 1 provides a summary of the model/particle parameters used. The terms of geometrical anisotropy and mechanical anisotropy have been commonly used to distinguish the two different natures of anisotropy in granular materials. For a spherical granular assembly, the geometrical anisotropy is usually described by the following fabric tensor (Satake, 1982):

$$\phi_{ij} = \langle n_i n_j \rangle \tag{1}$$

where n_i is the i-th component of the unit vector along the contact direction. The deviatoric invariant of ϕ_{ij}, A_c, is commonly used to denote the magnitude of anisotropy contributed by particle contacts:

$$A_c = \sqrt{3\phi'_{ij}\phi'_{ji}/2} \tag{2}$$

Meanwhile, it has been recognized that the nonlinear deformation behavior within a granular system, in form of force chain network, contribute considerably to the anisotropic behavior of the material. The anisotropic force chain network is largely formed by linear/nonlinear inter-particle forces transmitted at the contact points, along both the normal and tangential contact directions (in some cases, contact moments may be important but will not be considered here). This source of anisotropy, commonly termed as mechanical anisotropy, can be accounted by using two additional tensors χ^n_{ij} and χ^t_{ij}, defined in an analogous way to Eq. (1).

$$\chi^n_{ij} = \left\langle f^n n_i n_j \right\rangle / \left\langle f^n \right\rangle, \quad \chi^t_{ij} = \left\langle f^t t_i n_j \right\rangle / \left\langle f^n \right\rangle \tag{3}$$

Likewise, their deviations A_n and A_t are used to denote the amplitudes of the normal and tangential force anisotropy,

Table 1. Material properties.

Particle radius	Young's modulus	Poisson's ratio	Density	Frictional coefficient	
				Static	Dynamic
0.2 mm–0.6 mm	80 GPa	0.25	2700 kg/m^3	0.6	0.5

$$A_n = \sqrt{3\chi^{n}_{ij}\chi^{n}_{ji}/2}, \quad A_t = \sqrt{3\chi^{t}_{ij}\chi^{t}_{ji}/2} \tag{4}$$

where the superscripts n and t denote normal and tangential components of the quantities; t_i is i-th component of tangential unit vector and $n_i t_i = 0$.

The stress parameters used here are mean normal stress p and the deviatoric stress q, which are calculated from the stress tensor as defined by Christoffersen et al., (1981):

$$\sigma_{ij} = \sum f_i^c d_j^c / V \tag{5}$$

where V is the total volume of the assembly. f^c is the contact force, d^c is the inter-center vector joining the centers of the two particles at contact. Then p and q are defined as: $p = \sigma_{ii}/3$, $q = \sqrt{3\sigma'_{ij}\sigma'_{ij}/2}$.

3 RESULTS AND DISCUSSION

Fig. 1 shows the typical results under undrained triaxial compression, where the initial consolidation pressure has been fixed at 200 kPa and three packings with different initial void ratios have been used $e_0 = 0.57$, 0.64 and 0.72. In the case of $e_0 = 0.57$ denoted by the dotted red curve, a constantly hardening behavior is observed and the specimen can be loaded to state with relatively high mean normal stress level. For the case of $e_0 = 0.72$ which represents a relatively loose packing, the stress-strain relation (circle-marked curve in blue) demonstrate a mild strain-softening behavior. The mean normal stress decreases steadily during the loading until phase transformation state (denoted by the overturning point of the loading path) is reached. The case of $e_0 = 0.64$ denotes an intermediate packing between the first two and a behavior of slight softening and then followed by a regaining of strength (green curves with triangle markers) is observed. The influence of confining pressure on the soil response are shown in Fig. 2, for $p_0 = 300$ kPa, 200 kPa and 150 kPa, respectively. It is interesting to find that at $p_0 = 150$ kPa the sample experience liquefaction after a deviatoric strain of about 6% with all stresses approaching zero. The other two cases show general hardening.

The evolution of A_c, A_n and A_t over the loading course are plotted in Fig. 3 and Fig. 4. The contributions of weak and strong contact networks and as a whole system are comparatively depicted. As is shown in Fig. 3, in all cases, the degrees of anisotropy, in terms of A_c, A_n and A_t, remains low or close to zero during the loading course in the weak network. In contrast, the values of all three quantities increases steadily with the deformation level in the strong contact network and then stay at a constant peak of relatively high value. This appears to be supportive of the bimodal theory. However, a close look of Fig. 3c reveals that when the sand

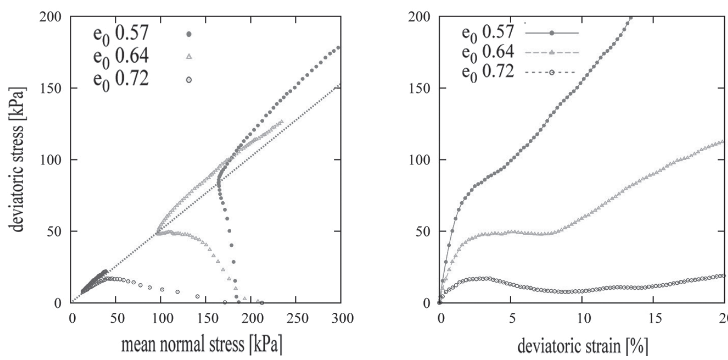

Figure 1. Effect of initial void ratio on the granular response under undrained shear (at a confining pressure of 200 kPa).

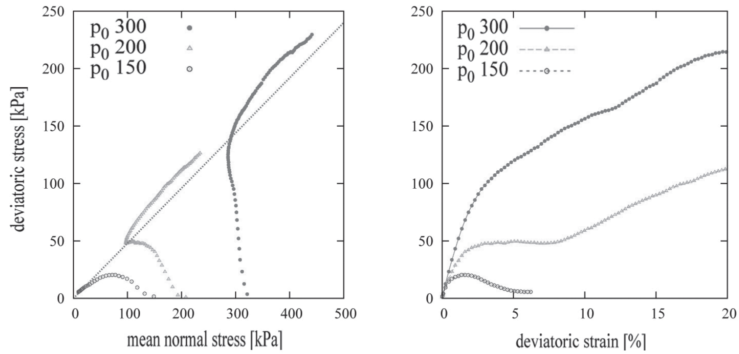

Figure 2. Effect of confining pressure on the granular response under undrained shear (e_0 fixed at 0.64 for all cases).

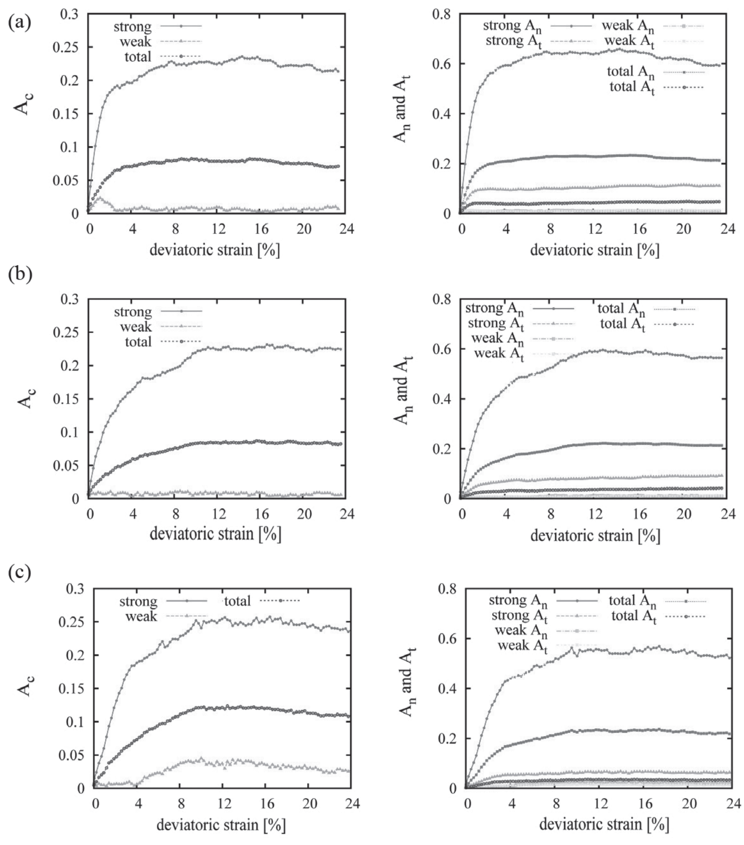

Figure 3. Evolution of geometrical and mechanical anisotropy with strain in packings with (a) $e_0 = 0.57$ (b) $e_0 = 0.64$ and (c) $e_0 = 0.72$ (p_0 is fixed at 200 kPa).

is packed relatively loose, certain degree of anisotropy will develop in the weak force network for A_c, which cannot be totally regarded as negligible. Compared to case (a) and (b), the total magnitude of A_c is also higher in the loose case of (c).

This is more obvious in the case when the sand enters the state of liquefaction, as shown in Fig. 4. The magnitude of A_c remains small initially when the deviatoric strain is below 2%. With further increase of strain level, A_c increases steadily until the liquefaction occurs.

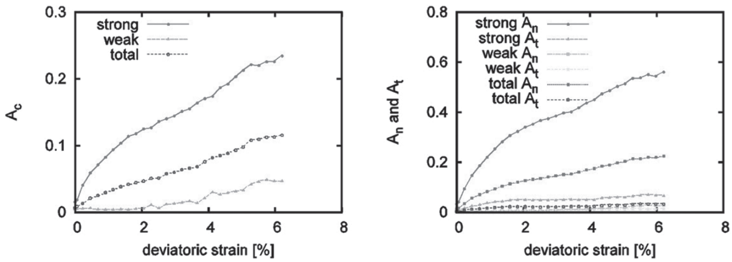

Figure 4. Geometrical and mechanical anisotropy in the packing at an initial void ratio $e_0 = 0.64$ with confining pressure 150 kPa (the sand is eventually liquefied).

This might imply that the weak network sustains significant deviatoric load during the process which may weaken its capability of acting as lateral support of the strong force columns to such an extent that liquefaction occurs. Meanwhile, we notice that during all the process the mechanical anisotropy in the weak network, in terms of A_n and A_t, remains small.

4 CONCLUSIONS

A 3D DEM study has been carried out to investigate the anisotropy and its evolution in a granular assembly under undrained shear. Geometric and mechanical anisotropy are carefully studied at various initial states, in relation with the bimodal character of stress transmission. It was found that the weak network can develop significant geometrical anisotropy under certain conditions and carry part of the deviatoric loads. Strain-softening and even catastrophic failures such as liquefaction may occur in this case.

ACKNOWLEDGEMENTS

This work was supported by RGC-HK (*623609*) and DAG-HKUST (*DAG08/09.EG04*).

REFERENCES

Azema E, Radjai F, Peyroux R, Saussine G (2007). Force transmission in a packing of pentagonal particles. Physical Review E 76: 011301.
Christoffersen J, Mehrabadi MM, Nemat-Nasser S (1981). A micromechanical description of granular material behavior. Journal of Applied Mechanics 48: 339–344.
Cundall PA, Strack ODL (1979). A discrete numerical model for granular assemblies. Géotechnique 29: 47–65.
Dorby R, Ng TT (1992). Discrete modeling of stress-strain behavior of granular media at small and large strains. Eng. Computation 9: 129–143.
Jefferies M, Been K (2005). Soil liquefaction: a critical state approach. Taylor & Francis.
Li XS, Dafalias YF (2002). Constitutive modeling of inherently anisotropic sand behavior. J. Geotechnical and Geoenvironmental Engineering, ASCE. 128(1): 868–880.
Mitchell JK, Soga K (2005). Fundamentals of Soil Behavior. John Wiley & Sons.
Oda M, Iwashita K (2000). Study on couple stress and shear band development in granular media based on numerical simulation analyses. Int. J. Eng. Sci. 38: 1713–1740.
Radjai F, Wolf DE, Jean M, Moreau JJ (1998). Bimodal character of stress transmission in granular packings. Physical Review Letters 80: 61–64.
Satake M (1982). Fabric tensor in granular materials. Deformation and failure of granular materials: 63–68.
Sitharam TG, Vinod JS, Ravishankar BV (2009). Post-liquefaction undrained monotonic behavior of sands: experiments and DEM simulations. Géotechnique 59: 739–749.
Wang Y, Alonso-Marroquin F (2009). A finite deformation method for discrete modeling: particle rotation and parameter calibration. Granular Matter 11: 331–343.